Solar Energy 218 (2021) 180–194

Contents lists available at ScienceDirect

Solar Energy

journal homepage: www.elsevier.com/locate/solener

Optimal control of switchable ethylene-tetrafluoroethylene (ETFE) cushions for building façades

Afshin Faramarzi, Brent Stephens, Mohammad Heidarinejad *

Department of Civil, Architectural, and Environmental Engineering, Illinois Institute of Technology, Chicago, IL, USA

ARTICLE INFO

Keywords:
Building energy performance
ETFE cushion, office building
Optimal control
Sequences of operation

ABSTRACT

Switchable ethylene-tetrafluoroethylene (ETFE) cushions with kinetic shading mechanisms are increasingly being used in building enclosures to dynamically control the transmission of solar and visible light. While buildings with switchable ETFE façades typically utilize simple Rule-Based logic to control their operation, this study uses a novel co-simulation approach to optimize the operation of switchable ETFE façades on two hypothetical office buildings in Chicago, IL. Four seasonally representative simulation days are used to demonstrate the approach. The daily source energy savings potential of the Optimal Control schedule is up to 8.2%, 11.1%, and 25.5% compared to Rule-Based, Always-Dark, and Always-Bright control strategies, respectively.

1. Introduction

The building sector is responsible for one third of global energy consumption (Berger & Mendes, 2017), with commercial and residential building energy consumption expected to grow ~1.9% annually (Pérez-Lombard et al., 2008). The building enclosure, which includes the walls, roof, foundation, windows, and shading devices that separate the conditioned interior environment from the exterior environment, impacts building energy consumption end-uses such as heating, cooling, and lighting, as well as indoor environmental quality (IEQ) (Sadineni et al., 2011). Heat transfer through walls and windows alone are estimated to account for a large proportion of heating and cooling energy needs in both residential (Huang et al., 1999) and commercial (Huang and Franconi, 1999) buildings.

A growing body of literature has demonstrated that novel envelope technologies and materials can offer new opportunities to reduce cooling, heating, and/or lighting energy end-uses in buildings. For example, one study demonstrated the use of passive strategies such as adding expanded polystyrene (EPS) thermal insulation, utilizing reflective coated glazing, adding overhangs, and white washing external walls resulted in 31.4% energy savings and 36.8% peak load savings in a high-rise building located in a hot and humid climate (Cheung et al., 2005). Another study showed that adding different thermal insulation to the walls, roofs, and floor reduced total energy consumption by 20–40%, while reducing air infiltration resulted in another 20% of energy savings (Chan and Chow, 1998). Another study demonstrated the effectiveness of a using completely delignified wood as a multifunctional, passive radiative cooling material composed of cellulose nanofiber bundles that reflects solar radiation up to 96% (Li et al., 2019). Simulations indicated that an average of ~30% cooling energy savings can be obtained for older midrise apartment buildings and an average of ~20% cooling energy savings is feasible for new midrise apartments. There are also other studies that used intelligent control of renewable energy power generators applied for grid-interactive buildings (Mu et al., 2018, 2020).

In addition to largely static building enclosure materials and technologies, architects and engineers have been designing, manufacturing, and testing smart (i.e., dynamic) building enclosure technologies to reduce thermal loads, provide thermal isolation, harvest energy, and/or improve IEQ (Menéndez et al., 2018). Dynamic building envelopes have the ability to modify their properties to meet energy efficiency goals, meet IEQ requirements, and interact with the electrical grid (DOE, 2019; Tang et al., 2018). These dynamic building enclosure technologies mostly operate under time-varying operation based on the interior and ambient conditions to achieve higher performance.

One promising trend in dynamic building envelope research is moving toward lightweight and transparent structures such as membrane and foil structures (Robinson-Gayle et al., 2001). Recent advances in sensors, actuators, and control systems have made active adaptable envelope systems applicable for use in buildings (Robinson-Gayle et al., 2001). These active systems are able to react instantly based on the feedback that they receive from indoor and ambient environmental conditions. Consequently, these technologies create opportunities to optimize thermal and optical performance of building envelopes and

* Corresponding author.
E-mail address: muh182@iit.edu (M. Heidarinejad).

https://doi.org/10.1016/j.solener.2021.01.059
Received 18 September 2020; Received in revised form 15 January 2021; Accepted 26 January 2021
Available online 11 March 2021

Nomenclature

Acronyms

BAS	Building Automation System
BPSO	Binary Particle Swarm Optimizer
CSV	Comma Separated Value
EPA	The U.S. Environmental Protection Agency
ETFE	Ethylene-Tetrafluoroethylene
EPS	Expanded Polystyrene
IDF	Input Data File
IEQ	Indoor Environmental Quality
LBNL	Lawrence Berkeley National Laboratory
NIST	National Institute of Standards and Technology
SHGC	Solar Heat Gain Coefficient
SOO	Sequences of Operation
TMY	Typical Meteorological Year
TOU	Time-of-Use
VCBT	Virtual Cybernetic Building Testbed

Variables

α	electricity site-to-source energy conversion factor
β	gas site-to-source energy conversion factor
L_{sch}	zone lighting illuminance
L_z	zone lighting
N	total number of simulations
Q_{clg}	cooling energy consumption
Q_{htg}	heating energy consumption
Q_{ltg}	lighting energy consumption
T_{sch}^{clg}	zone cooling temperature schedule
T_{sch}^{htg}	zone heating temperature schedule
T_z	zone temperature
$\vec{u}$	control trajectory
J	Joule
lx	lux (luminous flux)
°C	degree of centigrade

enhance the energy efficiency of buildings (Biloria and Sumini, 2009; Flor et al., 2018).

Ethylene-tetrafluoroethylene (ETFE) is one of the façade technologies that has gained interest due to its light weight and high daylight transmittance (Poirazis et al., 2009). When ETFE foils (sheets) are used on building façades, they are assembled into inflatable cushions. ETFE has comparable or even better optical, thermal, mechanical, and structural characteristics compared to glass structures. It is also lighter than glass. These key features together render ETFE popular among architects and engineers in recent years (Hu et al., 2017). A few prominent buildings worldwide, such as the Eden project in the UK, the Allianz Arena football stadium in Germany, the National Aquatics Center (Fig. 1a), the Changzhou Flora Expo in China (Fig. 1b), and the Kaplan Institute building in the U.S. (Fig. 1c) have utilized ETFE in their façades. Moreover, several prominent buildings worldwide have used switchable ETFE cushions with a kinetic shading mechanism that can be employed in roof and wall systems to dynamically control the transmission of solar and visible light, with the goals of saving energy, reducing peak power demands, and improving IEQ.

2. Literature review on ETFE façades

ETFE foils applied to buildings commonly consist of different configurations, ranging from just one layer to multiple layers (Flor et al., 2018). In multiple layer installations, multiple layers (i.e., ranging from 2 to 5) of ETFE foils are assembled to create a cushion with air pockets in between the layers. The cushions are then connected to air compressor (s) through a pipe network, which acts as a pneumatic system that stabilizes the air pressure. The air pressure is usually between 300 and 600 Pa and causes the inflated ETFE cushions to withstand external environmental forces such as wind. By controlling the air pressure between cavities of different ETFE foil layers, the position of the middle layer can be adjusted, for example by switching between dark mode (Fig. 2a) to bright mode (Fig. 2b) and vice versa. Since the layers are printed with inks and material additives, providing the ability to reflect/transmit light with different shapes and arrangements applied in different layers of the ETFE foil, the dark and bright positions yield different thermal and optical properties for the façade. It is noted that this pneumatically controlled mechanisms, which is commonly referred to as 'switchable' ETFE cushions, is a relatively new technology applied in only a small number of buildings worldwide (Flor et al., 2018).

A growing body of studies has assessed the mechanical and structural performance of ETFE foils, for example, evaluating mechanical behavior of ETFE foils under uniaxial monotonic tension (Hu et al., 2017; Zhao et al., 2020), under tensile loading conditions (Charbonneau et al., 2014), and during the form-developing process (Zhao et al., 2016). A limited number of studies have assessed the performance of ETFE cushions in terms of reducing building energy end-uses and/or improving daylighting, including a few studies that have used building energy modeling to assess the performance of ETFE installed on building envelopes. For example, Cremers and Marx (Cremers and Marx, 2016) conducted a comparative analysis on new infrared (IR)-absorbing ETFE film with conventional silver printing ETFE foil for a hypothetical building with a dimension of 20 m width, 10 m length, and 5 m height with a total volume of 1,000 m^3 located in Stuttgart, Germany. They estimated that the cooling energy and heating energy savings are 5–8% and 6–7%, respectively. Cremers and Marx conducted another study (Cremers and Marx, 2017) to evaluate the energy performance of spatially transformed ETFE-foil (3D-foil). In a 3-D foil, the printing pattern is adjusted exactly to the sun position in the sky. The cooling

(a) *(b)* *(c)*

Fig. 1. ETFE structures: (a) National Aquatics Center (Cushion ETFE), (b) Changzhou Flora Expo (single layer ETFE) (adapted from (Hu et al., 2017)), and (c) Kaplan Institute building (four layers switchable ETFE cushion).

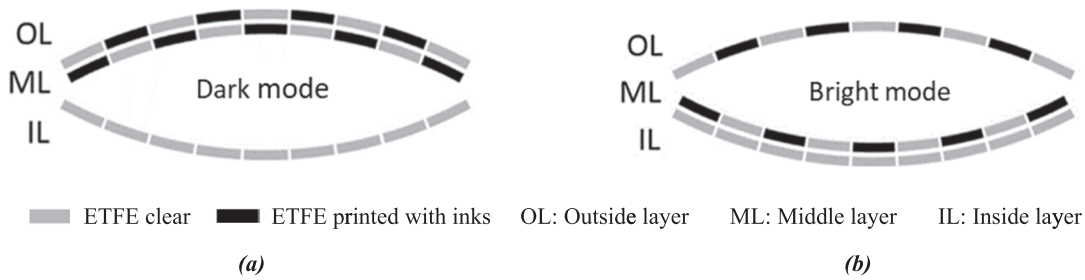

Fig. 2. (a) Dark and (b) Bright mode of switchable ETFE with three layers (figure adapted from Flor et al., 2018).

energy savings of a new 3D foil compared to a simple one-layer ETFE foil for the same building as the previous study was estimated as 69%. In order to have the most savings, the pattern in 3D foils must be printed based on the sun position in each project, which presents a limitation to the practical use of 3D foils. In their case, the optimal printing pattern was estimated by the sun position in Stuttgart, Germany.

Flor et al. (2018) investigated the energy savings potential of a building with different frit patterns printed on switchable ETFE cushions and compared it to traditional clear and reflective glazing. They estimated an annual energy savings potential (for heating, lighting and cooling end-uses) of about 45% for a switchable ETFE cushion compared to reflective double-glazing material. They also estimated that 65% more hours of useful daylight can be obtained in spaces covered by ETFE compared to reflective glazing. Afrin developed a simple simulation model for the heat transfer through the ETFE structures and then validated and calibrated the model by comparing it with measured data from test rigs and a case study building (Afrin, 2016).

While these existing studies show promise for energy savings potential, and ETFE cushion façades have already been built in several locations globally, buildings with switchable ETFE façades typically utilize fairly simple Rule-Based logic to control their operation. ASHRAE Guideline 36, which aims to summarize a list of best practices for the sequences of operation (SOO) for buildings, does not currently include any recommendations for these façade types (ASHRAE, 2018). To the best of our knowledge, there have not been any studies that have explored optimal operation or control strategies for switching ETFE façades. Therefore, this study seeks to explore optimal dynamic control strategies for actively interacting with the interior and ambient environments and varying the thermal and optical performance of ETFE cushion façades to reduce building energy and improve daylighting in hypothetical case study buildings. We use a co-simulation approach to optimize the operation of ETFE façades for two hypothetical office buildings in Chicago, IL USA using a set of practical constraints.

3. Methodology

The problem considered here is an optimal control problem, discretized in time. The problem is defined to find the control trajectory of ETFE status in three building directions (east, west, and south). Considering the discretized optimal control problem, taking into account each control node (time) as design variables, along with assuming two switching ETFE status (i.e., either dark or bright) as the domain of design variables, we convert the subject to a non-linear binary optimization problem. For solving this problem, we employed an advanced version of swarm intelligence binary optimizer (BPSO) with V-Shape transfer function.

3.1. Case study building energy models

Two hypothetical office buildings are considered in this study. Their areas are similar to U.S. Department of Energy (DOE) Reference buildings (Deru et al., 2011) for small and medium size office buildings. However, they differ from the reference buildings in other ways. For example, in order to maximize the effects of the ETFE cushion and to more accurately represent real installations, we use a 95% window-to-wall ratio for the case study buildings. To reduce computational run time, we consider only 5 thermal zones. The building schedules and other construction properties are modeled as the ASHRAE 189.1-2009 High-Performance buildings standard available in the OpenStudio library (ASHRAE, 2009).

The building energy model simulation engine is EnergyPlus V.9.1.0 for optimization purposes (Ellis et al., 2008). The initial modeling was accomplished by OpenStudio (V2.8.0). Fig. 3 shows the schematic view of these buildings. The small size building is considered as core-perimeter zone with 1 core thermal zone and 4 perimeter thermal zones with in total 5 thermal zones. It has one floor with an area of 508.7 m^2 with a core zone area of 107.4 m^2 and each perimeter zone area of 100.33 m^2. The model is considered as square with equal width and length of 22.6 m along with 3.05 m height. The depth of perimeter zones in each model is considered as 6.1 m. The zones are separated with internal partitions, with the lines shown on the roof of the building in Fig. 3. The HVAC system is considered as ideal air load system with dual thermostat setpoint schedule for the small office building located in Chicago, IL. The heating temperature setpoint is set to 21 °C from 6 am to 10 pm during occupied times with a temperature setback of 15.6 °C for unoccupied times. The cooling temperature setpoint is set to 24 °C from 6 am to 10 pm during occupied times with a setback of 26.7 °C for unoccupied times. For daylighting control, the setpoint is fixed at 500 lux for each zone, referenced by a node. As seen in Fig. 3, the original models are revised with the exterior side of perimeter zones considered as ETFE by modeling it as window in the initial design. All the thermophysical properties and HVAC system configuration for the medium size office building (Fig. 3a) are the same as the small office building (Fig. 3b), except the geometry. The medium size office has three floors, with each floor of 1,618.7 m^2, including a core zone with floor area of 786.3 m^2 and four perimeter zone with the floor area of 208.1 m^2 for each zone. This layout results in a square shape building with a total floor area of 4,856.1 m^2 with three floors.

We assume the building uses the Texlon® "Vario" ETFE system, which is a three-layered pressure inflated panel. The interior and exterior layers have a pattern printed on their inward facing sides, and dark and bright conditions are adjusted by pushing the printed middle layer toward the interior and exterior layers. Based on the definition from the manufacturer, Vector-foiltec, the print pattern combinations are SQM 200-197:45 dark (Maywald, 2019). Table 1 shows the optical and thermal properties of this system under the bright and dark modes, taken from (Maywald, 2019). Relevant thermal and optical properties include the transmittance, reflectance, and absorptance for ultraviolet (UV), visible, and solar light, shown separately for the bright and dark modes of the ETFE cushion. Visible properties provide information needed to design lighting fixtures while solar properties assist designers in estimating the potential impact of the façade heating and cooling loads. Table 1 also presents thermal properties including the Solar Heat Gain Coefficient (SHGC), which characterizes the amount of heat gain achieved by solar radiation through the ETFE cushion, the Shading Coefficient (SC), which characterizes the amount of solar heat gain of a

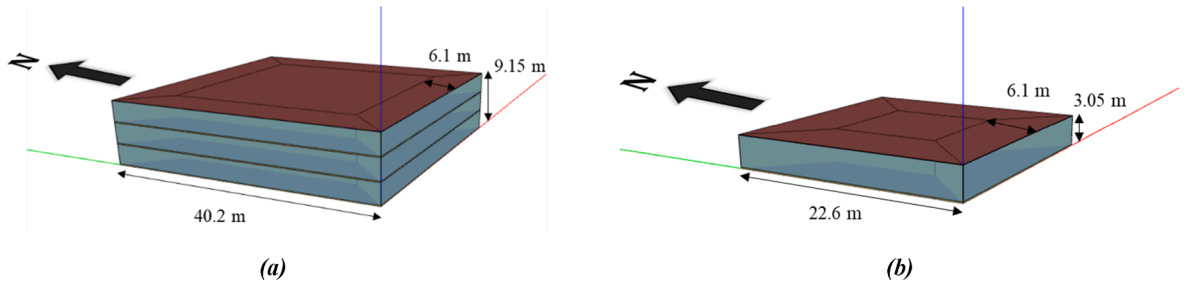

Fig. 3. Schematic view of the modified DOE Reference office building models: (a) medium size and (b) small size.

Table 1
Thermal and optical properties of the Bright and Dark modes of switchable ETFE cushions.

Texlon® Vario	Bright			Dark		
	UV light	Visible light	Solar light	UV light	Visible light	Solar light
Transmittance	15%	26%	26%	5%	9%	10%
Reflectance	14%	40%	38%	14%	53%	52%
Absorptance	71%	34%	35%	81%	38%	39%
g-value/SHGC	0.37			0.14		
SC	0.42			0.16		
U-value (W/m^2-K)	2.78			2.78		

specific fenestration material compared to the standard clear float glass, and the U-value, which characterizes the heat transfer transmittance of the material.

3.2. Control strategies

We consider four control strategies in this study: (1) Always-Dark, (2) Always-Bright, (3) Rule-Based, and (4) Optimal Control. The ETFE operation is assumed to be the same for all floors facing the same direction. For example, for the east side, all the ETFE in three floors of the medium size office building are assumed to be controlled by one schedule and controller. This applies for the south and west sides as well, although different facing façades are assumed to operate independently. The north side is not connected to any controller and is assumed to be always bright due to the lack of direct sunlight in the studied latitudes. For both building case studies, the SOO for each control strategy is as follows:

- Always-Dark: ETFE actuators are always acting, which results in constant dark status regardless of the time of day, occupancy, or orientation of the space;
- Always-Bright: ETFE actuators are never acting, which results in constant bright status. Similar to the Always-Dark strategy, the time of day, occupancy, and orientation of the spaces do not impact ETFE operation;
- Rule-Based: ETFE actuators act when the outdoor air temperature is above 15.6 °C. This rule is inspired by the SOO that is currently being applied in the Kaplan Institute building (Fig. 1c). Therefore, we consider this as a simple Rule-Based control to be compared with the Optimal Control. The temperature of 15.6 °C is based on the building automation system (BAS) parts of architectural/construction drawing of the building with considering a few simplifications; and
- Optimal Control: ETFE actuators will act based on the optimal schedule derived from minimization of total daily heating, cooling, and lighting energy consumption.

In order to evaluate and compare the performance of these control strategies during different days, a day in a shoulder season (September 30) and three solstice and equinox days (March, June, and December 21) are selected for simulation. The majority of the analysis and results are conducted on the shoulder season day (September 30) to demonstrate the approach because shoulder seasons provide the most opportunity for optimal control of dynamic façades due to larger diurnal fluctuations in ambient conditions than solstice or equinox days. Only day-long simulations are utilized because of the computational time required for annual analysis and because day-long simulations provide clearer insight into dynamic operational characteristics.

3.3. Optimization algorithm

There are many problems that intrinsically have the nature of discrete binary search space. The problem such as dimensionally reduction and feature selection can be categorized as binary problems (Pal and Maiti, 2010; Zeng et al., 2009). The problem with continuous search space can also be converted to a binary problem type witch has own its structure with some limitation (Mirjalili and Lewis, 2013). A binary search space can be imagined as a hypercube in which the search agents are only allowed to shift to the close/far corners of this hypercube with selecting various number of bits (Kennedy and Eberhart, 1997). It is possible to design the binary version of originally continuous optimization method (Emary et al., 2016; Kennedy and Eberhart, 1997). The continuous optimization methods are revised in structure with sometimes considering proper transfer function to map the search agent updates into the domain dealing with only two numbers of “0” and “1”. In Particle Swarm Optimization (PSO), the transfer function is responsible to connect a link between position and velocity of the particles. The velocity values are converted to probability values for updating the positions of the particles. The traditional PSO uses sigmoid function as transfer function of velocities into probabilities. Since the sigmoid transfer function is like the word “S”, a group of sigmoid functions with shape of “S” are called an S-shaped family of transfer functions (Mirjalili and Lewis, 2013). Another family of transfer functions, the V-shaped family, have also shown better performance than the S-shaped family (Mirjalili and Lewis, 2013). One of the recently developed functions of V-shape family has shown more promising performance compared to others in this class (Mirjalili and Lewis, 2013). The reason for better performance of this class of functions is because of its equal behavior (resulting in equal probability) with status updating of the design variables that have the same absolute velocity. Since the optimal control problem of ETFE cushion envelope is a binary problem, we used the binary version of PSO with V-shape transfer function for the optimization purpose.

3.4. Co-simulation architecture

We used a “static” co-simulation architecture to couple the optimizer (MATLAB) and simulator (EnergyPlus). In a static co-simulation, data is exchanged just one time between the clients at each iteration/timestep (Zhai, 2003). In this work, the optimizer (MATLAB) is responsible for writing the optimal schedule of ETFE status into a CSV (Comma-Separated Value) file in an iteration, which serves as the input for the

simulator (EnergyPlus). Conversely, the simulator (EnergyPlus) is responsible for writing the results of heating, cooling, and lighting loads as inputs for the optimizer (MATLAB) in an iteration. Consequently, the input of one client works as the output for the other client. The data are exchanged at each timestep (which in this case is each iteration). To achieve this, a syntax in MATLAB called "system" is used to call EnergyPlus. This syntax calls the operating system to execute a specified command. The defined command here to execute EnergyPlus entails a character vector that includes three strings. The first string is the directory address of the executable EnergyPlus file in the command prompt called "RunEplus". The second string includes the IDF information that contains the name of the IDF file along with its directory. The third string entails the weather data information (i.e., file name and its directory). The "system" will return the "status" and "cmdout" of the execution. The "status" indicates if the command completed successfully or not and the "cmdout" returns the output of the command. Fig. 4 shows the architecture of the data exchange in more detail.

As mentioned, we used OpenStudio for the initial modeling of our case study; however, OpenStudio in the co-simulation architecture is never actually called and run. After revising the geometry and assigning HVAC systems and construction materials in OpenStudio, we run the initial simulation from OpenStudio to generate the EnergyPlus input data file (IDF). Then, the IDF file is employed in the proposed co-simulation architecture. However, before using the IDF file, we need to modify it and prepare it for data exchange ability. The modification steps are as follows:

- Schedule type limit: defined the limit of ETFE operation status as discrete numeric type define by 0 and 1;
- Construction: Defined two status of ETFE as dark and bright mode;
- Window material: Assigned optical and thermal properties of the dark and bright ETFE status previously defined in "Construction";
- Daylighting reference point: Defined the reference point for daylighting control in each zone;
- Daylighting control: Assigned the reference point defined in previous section along illuminance setpoint for daylighting control;
- Schedule-file: defined the schedule file name for each orientation of east, south, and west; and
- Window shading control: Assigned the shading type as "Switchable Glazing" and shading control type as "on if schedule allows".

Within EnergyPlus, we modeled the ETFE dark and bright conditions simply as two different window types with different optical/thermal properties and used a switchable glazing control type to switch between ETFE conditions according to the external schedule file in a CSV format indicating ETFE operation mode with binary numbers (0 and 1). The switching mechanism is first carried out by assigning the dark status in "window control shading" and bright status in "construction" tabs in the IDF editor section on EnergyPlus. Then the binary number of 0 and 1 in schedule CSV file is used to actuate the status as either "off" (as bright mode) or "on" (as dark mode), respectively. Interested readers can visit the EnergyPlus Input-Output Reference Manual for more details (EnergyPlus, 2000).

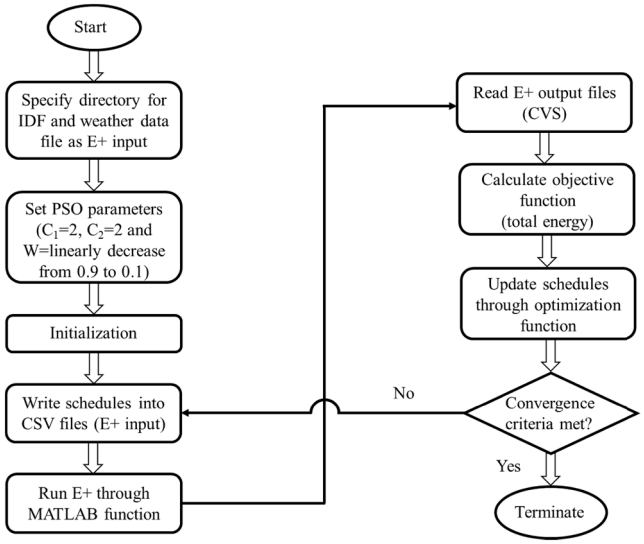

Fig. 4. Co-simulation architecture of simulator-optimizer platform.

3.5. Objective function and design variables

The objective function considered in this study is the total daily source energy use for heating, cooling, and lighting. Cooling and lighting both use electricity and heating uses natural gas. Site to source energy conversion factors are considered as 3 for electricity, as an average of value derived from the National Renewable Energy Laboratory (NREL) (Deru and Torcellini, 2007) and the US Environmental Protection Agency (EPA), and 1.05 for natural gas per the US EPA's conversion table. The design variables (optimal control nodes) are defined as the ETFE status in each of the east, south, and west directions. The execution horizon for the optimal control problem is considered from 5 am to 8 pm, with two control nodes in each hour and each direction of east, south, and west. In other words, we assume that the ETFE status can be switched every 30 min, which results in 30 control nodes in each direction between 5 am to 8 pm, and 90 control node/design variables for the problem in total. Thus, the optimal control of ETFE is mathematically formulated as Equation (1):

$$\textit{Minimize} \quad J(\vec{u}_E, \vec{u}_S, \vec{u}_W) = \sum_{i=1}^{N} \alpha\left(Q_{clg_i} + Q_{ltg_i}\right) + \sum_{i=1}^{N} \beta Q_{htg_i}$$

$$\textit{Considering} \begin{cases} \vec{u}_E \in \{0,1\}^{30} \\ \vec{u}_S \in \{0,1\}^{30} \\ \vec{u}_W \in \{0,1\}^{30} \end{cases}, \quad \textit{and} \quad \textit{subject to} \begin{cases} T_z \in [T_{sch}^{htg}, T_{sch}^{clg}] \\ L_z \in [L_{sch}] \end{cases} \tag{1}$$

where $\vec{u}$ is the control trajectory, $N$is the number of total simulation time steps in a specified day (the time step set 10 min as the EnergyPlus default recommendation), α and β are the site-to-source energy conversion factors for electricity and heating, respectively, Q_{clg}, Q_{ltg} and Q_{htg} are the site cooling, lighting, and heating energy consumption (J), respectively, $T_z$is the zone temperature (C), and L_z is the zone lighting illuminance (lux). Zone temperatures and zone lighting illuminance are both constraints for the minimization problems.

4. Results

Detailed results from the four simulated control strategies are explored for a single day representative of a typical shoulder season in Chicago, IL (September 30). A shoulder season timeframe is considered because it captures days when the outdoor temperature is both above and below the outdoor temperature assumed to trigger action in the Rule-Based control strategy (15.6 °C), which allows for comparison among all four of the simulated strategies. For example, if during a summer day the outdoor air temperature fluctuates from 20 °C to 30 °C, two of the comparison control strategies (Rule-Based and Always-Dark) would yield the same results.

Fig. 5 shows the outdoor dry bulb temperature, direct solar radiation flux, and sky clearness from the typical meteorological year (TMY3) weather file on the simulated day (EnergyPlus, 2020). Fig. 5a shows that the maximum outdoor air temperature is around 19 °C at 1:00 pm while the minimum is 8 °C at 10:00 pm. Fig. 5b shows the sun rises at 6:00 am and sets at 5:30 pm, with two sudden decreases around 7:30 am and 11:30 am due to cloud cover (Fig. 5c).

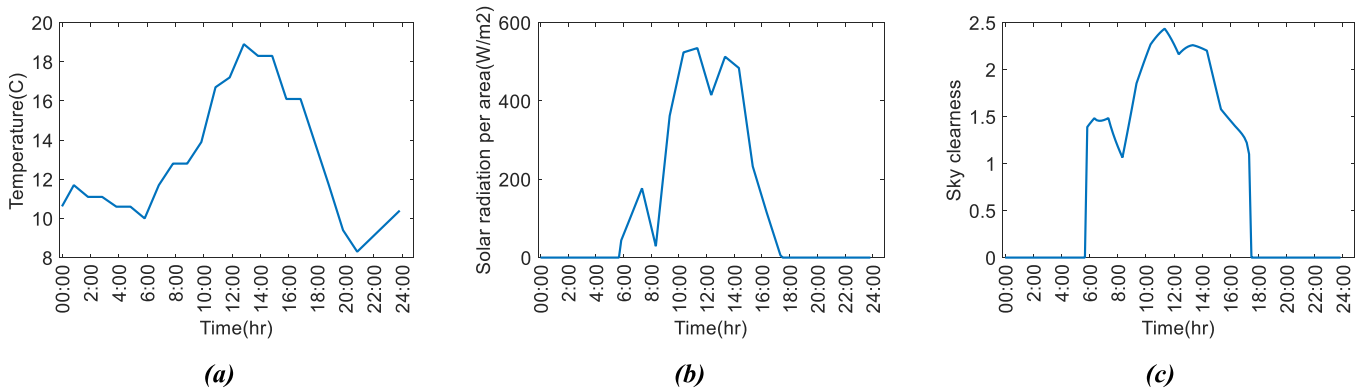

Fig. 5. Outdoor conditions on the simulated day in September: (a) outdoor air temperature, (b) solar irradiation, and (c) sky clearness.

4.1. Small office building

The ETFE variable considered in this study is binary, meaning that the ETFE system can switch between either of two extreme conditions: dark or bright. Fig. 6 shows the assumed schedules for Always-Bright operation (Fig. 6a), Always-Dark operation (Fig. 6b), and Rule-Based control operation (Fig. 6c). The Rule-Based control strategy is applied to all directions at the same time; when the outdoor temperature increases beyond 15.6 °C (e.g., from 10:30 am to 5:00 pm on the simulation day, as shown in Fig. 5a), the ETFE cushion switches to dark status for all sides. This simple Rule-Based control is directly informed by discussions with facility managers at the Kaplan Institute building who operate an ETFE cushion façade.

Fig. 7 shows lighting, cooling, and heating energy end-uses in the Always-Bright mode of operation during the September simulation day. Lighting energy use in the core zone is higher than the other zones, with a peak energy consumption around 550,000 J during a 10-minute simulation interval from 8:00 am to 5:00 pm. Since the ETFE is always bright, all the thermal zones on the perimeter need approximately the same pattern of lighting energy, with a minimum energy consumption around 150,000 J during a 10-minute interval within that period. The reason that the perimeter zones still need lighting with the ETFE cushion operating in the Always-Bright mode is that in order to control the light, we used continuous dimming control in EnergyPlus. Based on the default recommendation of EnergyPlus, we set the minimum input power fraction (the lowest power the lighting system can dim down to, expressed as a fraction of maximum input power) to 0.2 and the minimum light output fraction (the lowest lighting output the lighting system can dim down to, expressed as a fraction of maximum light output) to 0.3. Lighting energy use increases for all perimeter zones starting around 2:30 pm because of a decrease in solar light due to the overcast sky at that time, as observed in Fig. 5b and c. Moreover, the east side requires additional lighting energy earlier in the day than the south and west zones, which is consistent with solar geometry patterns at this latitude. The south-facing perimeter zone has the highest cooling energy consumption due to more solar gain that it receives during the entire day (Fig. 7b). Fig. 7c shows that heating energy consumption for all zones are more or less the same, occurring only in the early morning and nighttime in this shoulder season day due to decreases in outdoor temperature, as shown in Fig. 5a.

Fig. 8 shows lighting, cooling, and heating energy end-uses in the Always-Dark mode of operation during the September simulation day. As shown in Fig. 8a, lighting energy consumption in Always-Dark mode is higher than in the Always-Bright mode, especially on the east, west, and south perimeter zones. Lighting energy consumption for the east and west zones intuitively intersect at the middle of the day, while the south zone is lowest. Fig. 8b shows that there is no cooling required for the east, north, or core zones at any time, while the cooling energy consumption is considerably lower than the Always-Bright mode for the south and west side zones. Fig. 8c shows that the heating energy consumption required in the east, west, and south zones is similar to, albeit a little higher than, the Always-Bright mode. The reason for minor differences is because heating needs are only from 6:00 am to 9:30 am and 6:00 pm to 10:00 pm, when solar radiation is minimal.

Fig. 9 shows lighting, cooling, and heating energy consumption for the Rule-Based control strategy applied uniformly to all façades on the September simulation day. Referring back to Fig. 6c, from 10:30 am to 5:00 pm, the ETFE façade is in dark mode operation (with ambient temperatures above 15.6 °C), and in bright mode the rest of the time. Consequently, Fig. 9a shows that the lighting energy use in each zone in Rule-Based control operation follows the same trend of the lighting load in Always-Dark mode from 10:30 am to 5:00 pm, while in other hours it follows the trend of Always-Bright mode. Fig. 9b shows the cooling energy consumption for this control strategy. As expected, the cooling

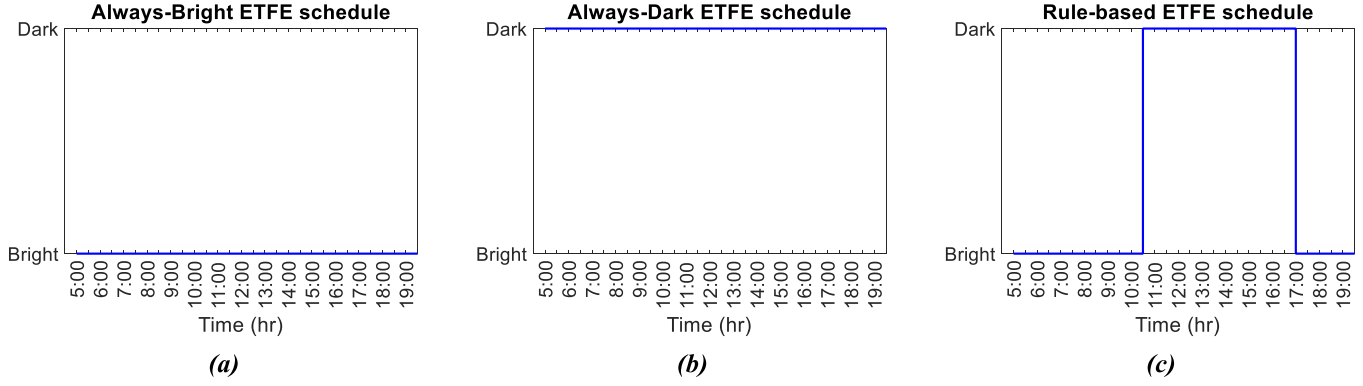

Fig. 6. Schedule of ETFE for (a) Always-Bright, (b) Always-Dark, and (c) Rule-Based operation on the September simulation day.

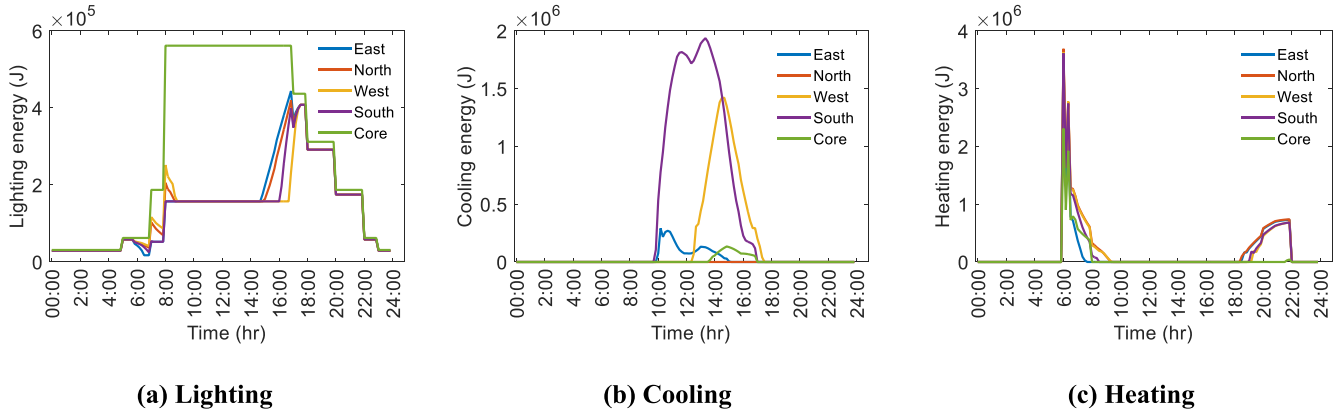

Fig. 7. Site energy consumption of the small office building using the Always-Bright strategy during the September simulation day: (a) lighting, (b) cooling, and (c) heating.

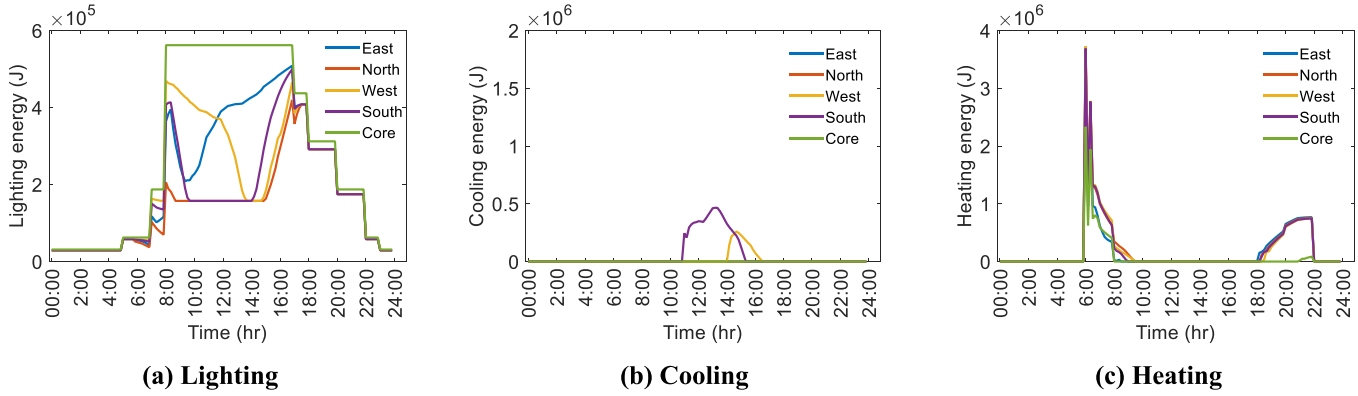

Fig. 8. Site energy consumption of the small office building using the Always-Dark strategy during the September simulation day: (a) lighting, (b) cooling, and (c) heating.

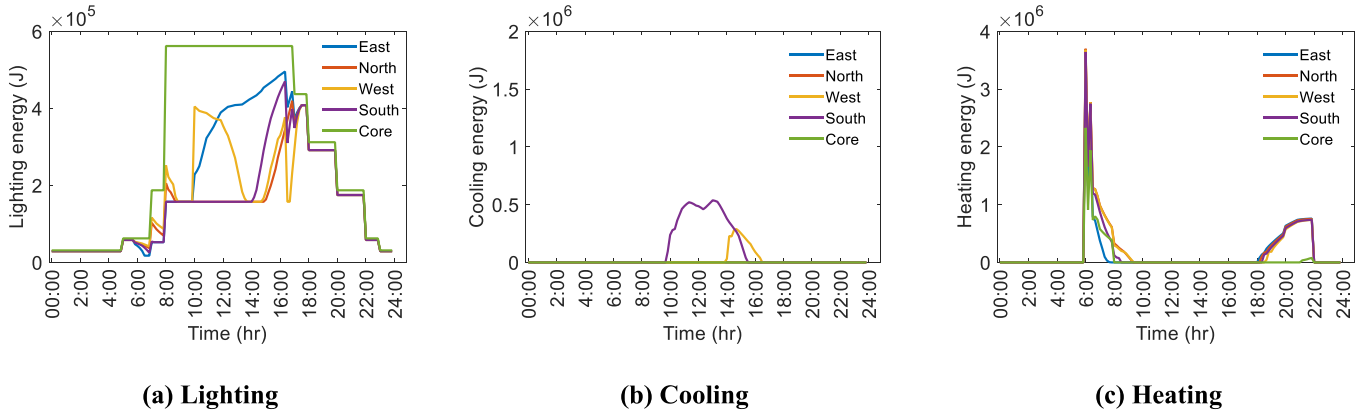

Fig. 9. Site energy consumption of the small office building using the Rule-Based control strategy during the September simulation day: (a) lighting, (b) cooling, and (c) heating.

energy pattern is similar to the cooling energy pattern of Always-Dark mode operation (Fig. 8b), although the cooling load on the south-facing perimeter zone is slightly larger than Always-Dark because before 10:30 am, the ETFE is in bright mode, which allows transmitted solar radiation to heat the south zone, resulting in more cooling required for the zone subsequently. Fig. 9c also shows that heating energy consumption in each zone in the Rule-Based control strategy is similar to the Always-Bright mode, as heating is only required when Rule-Based control calls only for coincident bright mode.

Fig. 10 shows the resulting Optimal Control schedule for the east, south, and west ETFE cushion façades in the small office building during the September simulation day. Resulting time-varying estimates of lighting, cooling, and heating energy consumption under the Optimal Control strategy on the same simulation day are shown in Fig. 11. In the east perimeter zone, the ETFE façade is operated in bright mode from 30 min after sunrise (6:30 am) until 9:30 am to benefit from both daylighting and solar heating. From 9:30 am to 10:30 am, the east ETFE façade changes to dark status, when the optimizer determines that changing to dark status for a one-hour period would increase lighting needs but decrease cooling needs to a greater extent. From 10:30 am

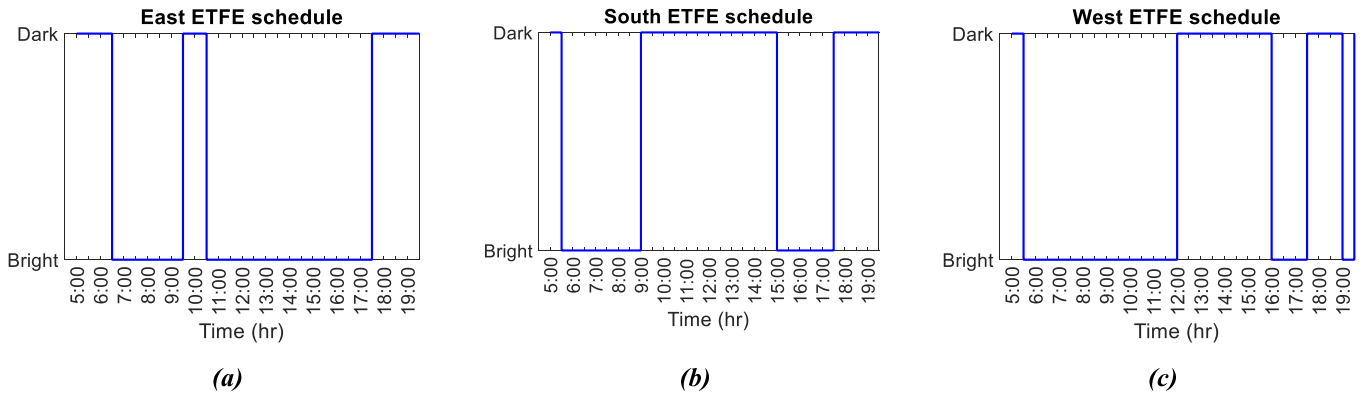

Fig. 10. Optimal Control schedule of ETFE status for three façades on the small office building during the September simulation day: (a) east, (b) south, and (c) west.

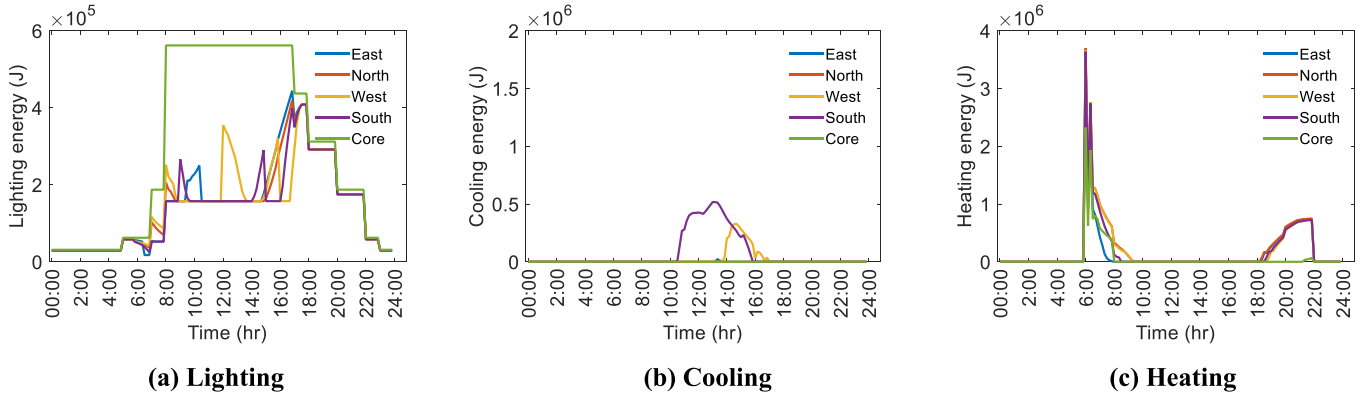

Fig. 11. Site energy consumption of the small office building using the Optimal Control strategy during the September simulation day: (a) lighting, (b) cooling, and (c) heating.

until sunset at 5:30 pm, the east ETFE façade remains in bright mode operation to benefit from daylighting without intense solar radiation. After 5:30 pm, the ETFE façade changes again to dark mode. We also noticed that if the schedule would remain as bright after 5:30 pm, there would be a slight increase in heating energy because the ambient temperature keeps decreasing after 5:00 pm and keeping the ETFE in bright mode would affect the office by radiative heat transfer to the outside.

In the south perimeter zone, the ETFE façade is operated in bright mode from sunrise until 9:00 am to take advantage of natural daylighting, then it switches to dark status until 3:00 pm to decrease cooling energy needs. From 3:00 pm to 5:30 pm, the south façade again switches to bright status because solar radiation is not intense in the evening, so the cooling demand is not large, while lighting energy is minimized. For the west perimeter zone, the ETFE façade is operated in bright mode from sunrise until 12:00 pm. This duration is longer than the east and south faces because the west side does not face direct sunlight until afternoon. Therefore, the optimizer takes the most advantage of daylighting before noon without increasing the cooling energy beyond lighting saves. Subsequently, from 12:00 pm to 4:00 pm, the west ETFE façade changes to dark status in order to minimize cooling energy consumption (the peak cooling demand when the ETFE is in bright mode occurs at 2:40 pm, as shown in Fig. 7b). The west side ETFE façade then switches to bright mode from 4:00 pm to 5:30 pm, as solar radiation decreases, and the benefits of natural daylighting are greater than the impacts on cooling energy needs in that timeframe. Finally, after 5:30 pm, the ETFE cushion switches to dark status on all sides. Overall, the net impact of each control strategy on daily energy consumption is summarized in Section 4.3.

4.2. Medium office building

We considered the same core-perimeter zone concept for the medium size office building. In order to reduce computational run time, all three floors on each side were considered as one thermal zone. Therefore, we again have one core zone along with four perimeter zones, even in this larger case study. The core zone has a larger area and volume compared to perimeter zones. The lighting, cooling, and heating energy consumption for the two base strategies of Always-Bright and Always-Dark during the September simulation day are presented in Fig. 12 and Fig. 13, respectively.

Based on Fig. 12a, the lighting energy consumption of the core zone is considerably higher than the other zones. This is because this zone is not only larger than the other zones, but also because internal partitions that encircle the core zone prevent this zone from benefitting from any natural daylighting. Therefore, changing the status of ETFE will not have any effect on the lighting of core zone of medium office. It also applies for the small office, but in the small office, the core zone is not much larger than the perimeter zones, so the lighting energy required for the core zone in the medium size office is considerably higher than the lighting energy of the core zone needed in small office.

Fig. 12b presents the cooling energy consumption of each zone under Always-Bright operation. It is interesting to note that even though the core zone in the medium size office is larger than the other zones, the cooling energy consumption of the core and south-facing zones are competitive with each other due to high solar gains on the south side during the day. East, north and west side perimeter zones have lower cooling energy than the core and south side zones. Fig. 12(c) shows the heating energy for this mode of operation. In contrast to lighting and cooling, the core zone requires the lowest heating energy for this model

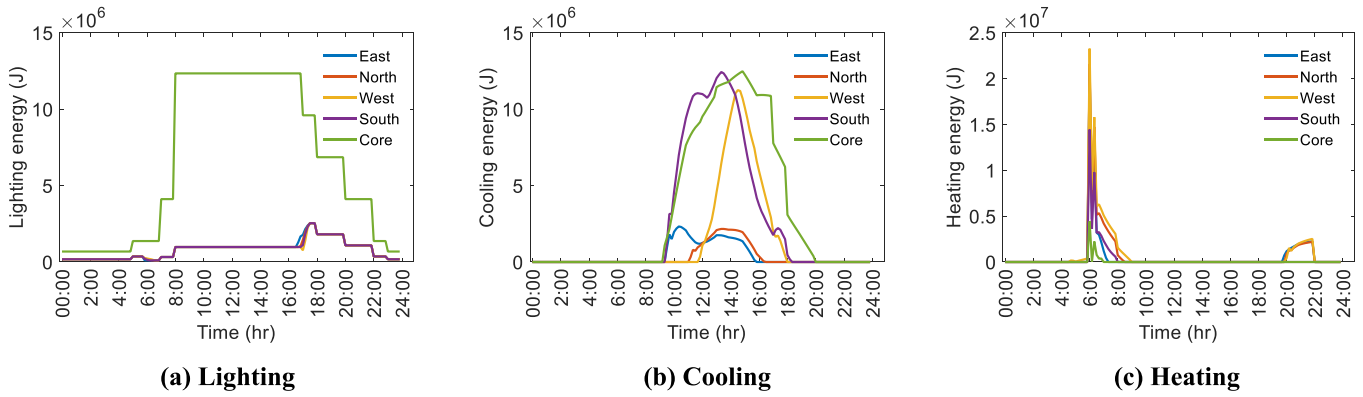

Fig. 12. Site energy consumption of the medium office building using the Always-Bright strategy during the September simulation day: (a) lighting, (b) cooling, and (c) heating.

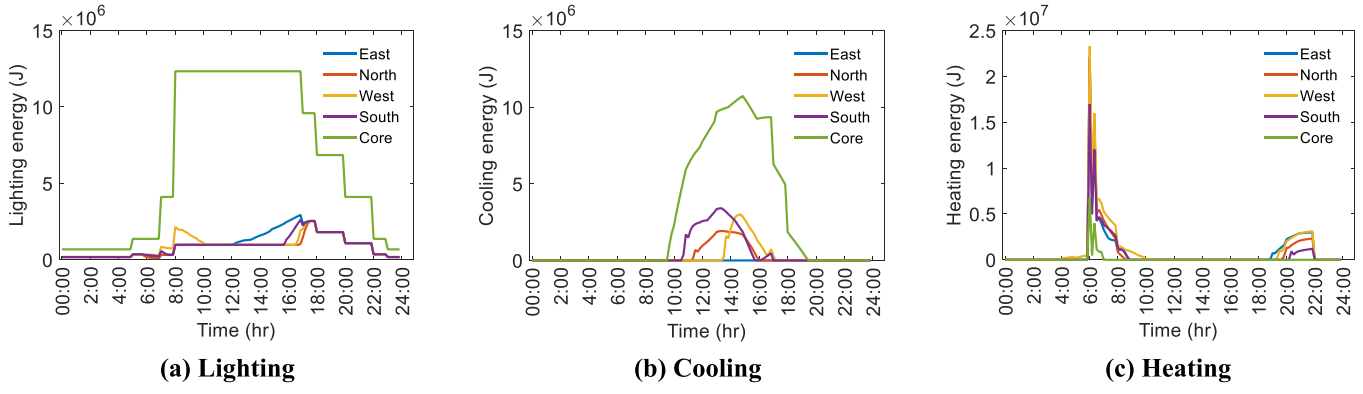

Fig. 13. Site energy consumption of the medium office building using the Always-Dark strategy during the September simulation day: (a) lighting, (b) cooling, and (c) heating.

because it is surrounded and thermally protected by the perimeter zones, with heat gains from people and equipment contributing to meeting heating needs. In this larger case study building, heating is only required during short periods of time in the morning and early night to satisfy the temperature setpoints.

Similarly, Fig. 13a depicts lighting energy use for the Always-Dark mode of operation during the September simulation day. The west, south, and east zones have higher lighting energy use in Always-Dark mode compared to the same zones in Always-Bright mode, while lighting energy use in the north and core zones are the same as in Always-Bright mode. Fig. 13b shows the cooling energy in the Always-Dark mode, where the loads in all zones except the core zone are substantially lower than in the Always-Bright mode. Fig. 13(c) shows that the heating energy use for all zones in Always-Bright mode are only slightly higher than in Always-Dark mode, for reasons similar to those explained for the small office building.

Fig. 14 shows the resulting optimal schedule for the east, south, and west ETFE cushion façades in the medium size office building during the September simulation day. The schedule for Always-Dark, Always-Bright and Rule-Based control are the same as Fig. 6. Fig. 15 presents lighting, cooling, and heating energy consumption for the Optimal Control strategy during the same simulation day.

Based on Fig. 14a, the ETFE façade on the east perimeter zone is in bright mode until 8:00 am to decrease heating energy and lighting

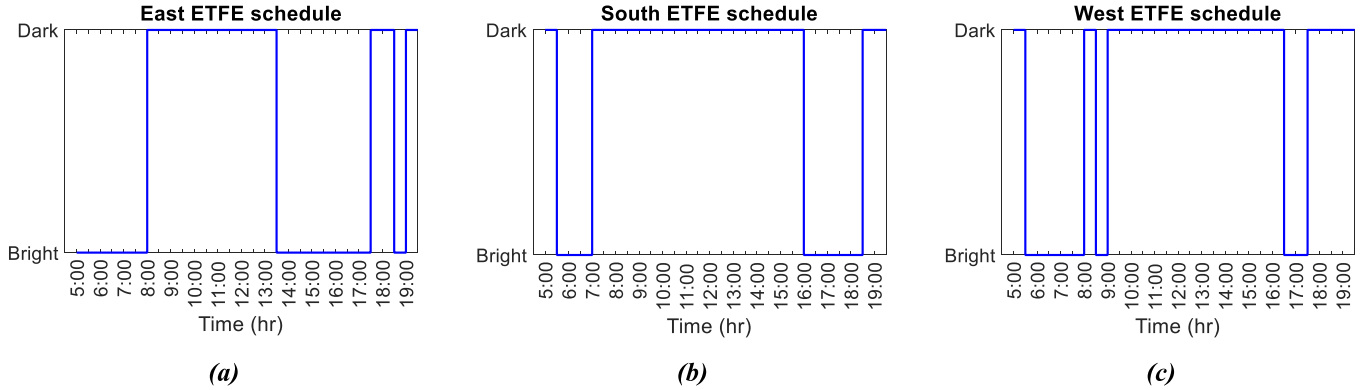

Fig. 14. Optimal Control schedule of ETFE status for three façades on the medium office building during the September simulation day: (a) east, (b) south, and (c) west.

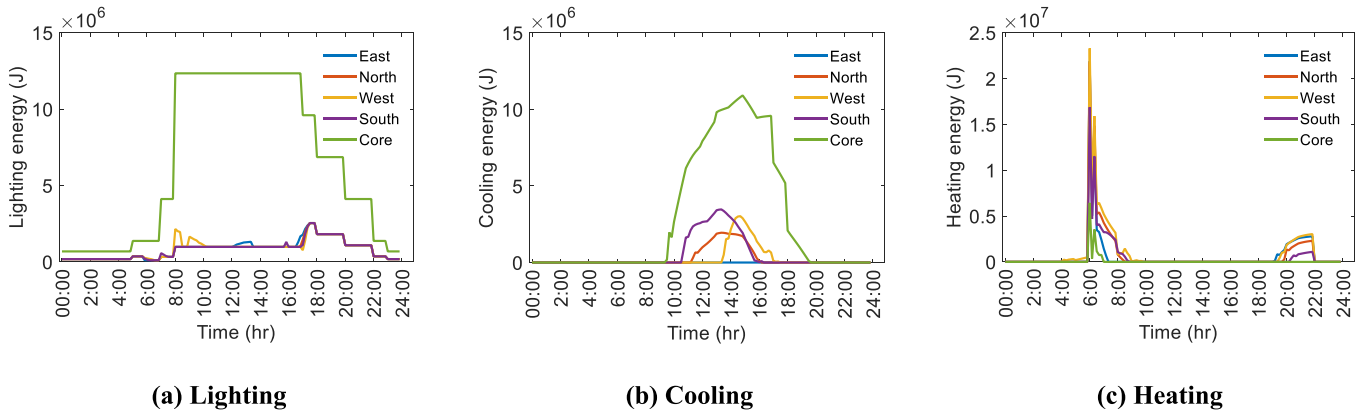

Fig. 15. Site energy consumption of the medium office building using the Optimal Control strategy during the September simulation day: (a) lighting, (b) cooling, and (c) heating.

energy needs in the morning, then it switches to dark mode until 1:30 pm. Based on Fig. 12b, if ETFE is in bright mode, the east zone requires cooling from 9:20 am until 4:00 pm. Therefore, this switch will decrease the cooling energy needs while increase the lighting energy needs, but in order to have lowest energy consumption, the optimizer identifies greater benefits in decreasing cooling energy needs. From 1:30 pm to 5:30 pm, the east ETFE façade is in bright mode to minimize lighting energy, which has greater benefits than decreasing concurrent cooling energy needs. For the south side, the ETFE façade is operated in bright mode from sunrise until 7:00 am to benefit lighting needs, then switches to dark status until 4:00 pm (near sunset), and then switches to bright until 6:30 pm. The reasons for these switches are the same as those discussed previously for the small office building. The west side operation is also similar to the small office building as well, albeit with shorter duration and a shift in hours of operation.

One of the major differences between the optimal ETFE schedule for the medium size office building and the small office building is that in the medium size office, the schedule in all directions tends to switch to the dark mode during most hours of the day. The reason is the sensitivity of the zones' cooling energy (except the core zone) to the different ETFE status (Fig. 12b and Fig. 13b), which results in the optimizer giving priority to cooling energy needs as the key load for optimization. We also observed that the cooling and lighting energy consumption of the core zone is much higher than the other zones and does not change with different ETFE operational modes.

4.3. Energy consumption and savings

Table 2 shows the estimated total daily source energy consumption for both building case studies for the September simulation day under each of the four ETFE cushion control strategies.

Table 3 shows the percentage source energy savings resulting from the use of the optimal ETFE cushion control strategy compared to the three other strategies for the September simulation day. The Optimal Control strategy resulted in total savings of 25.5%, 11.1%, and 8.2% compared to Always-Bright, Always-Dark, and Rule-Based control, respectively, for the small size office building. Similarly, the Optimal Control strategy resulted in total savings of 21.9%, 2.2%, and 3.7% compared to Always-Bright, Always-Dark and Rule-Based control, respectively, for the medium size office building. Intuitively, the reason that the energy savings potential of the Optimal Control strategy applied to the medium size office is lower than the small size office is because of the greater contribution of the core zone in the larger building, which is not affected by ETFE position.

Table 2
Total daily source energy consumption for small and medium size office buildings during the September simulation day under each of four ETFE cushion control strategies.

Total daily source energy consumption, J (kWh/m^2)		
Control Strategies	*Small size office*	*Medium size office*
Always-Bright	7.21×10^8 (0.393)	8.07×10^9 (0.450)
Always-Dark	6.04×10^8 (0.329)	6.44×10^9 (0.359)
Rule-Based	5.85×10^8 (0.319)	6.54×10^9 (0.365)
Optimal	5.37×10^8 (0.292)	6.30×10^9 (0.351)

Table 3
Total daily source energy savings from using the Optimal Control strategy compared to the three other strategies in the small and medium size office buildings during the September simulation day.

Total daily source energy savings (%)		
Optimal Control savings compared to the other strategies	Small size office	Medium size office
vs. Always-Bright	25.5%	21.9%
vs. Always-Dark	11.1%	2.2%
vs. Rule-Based	8.2%	3.7%

4.4. Other solstice and equinox days

In order to evaluate the effect of the ETFE Optimal Control strategy on building energy consumption patterns during other seasons, we ran simulations for three additional simulation days, including solstice days of June 21 and December 21, and the equinox day of March 21, each as representative days for summer, winter, and spring shoulder seasons, respectively. It is noted that we already discussed the detailed results of September 30, which is close to another equinox day of September 23.

Table 4
Total daily source energy consumption for the small and medium size office buildings under each of four ETFE cushion control strategies for the 21st of December, June, and March.

Total daily source energy consumption (J)						
Control Strategies	Small size office			Medium size office		
	Dec 21	June 21	March 21	Dec 21	June 21	March 21
Always-Bright	1.38×10^9	2.03×10^9	9.69×10^8	9.25×10^9	2.20×10^{10}	7.17×10^9
Always-Dark	1.48×10^9	1.56×10^9	1.02×10^9	9.77×10^9	1.80×10^{10}	7.27×10^9
Rule-Based	1.38×10^9	1.56×10^9	9.69×10^8	9.25×10^9	1.80×10^{10}	7.17×10^9
Optimal	1.38×10^9	1.53×10^9	8.73×10^8	9.25×10^9	1.78×10^{10}	6.50×10^9

This section briefly describes and analyzes the outcomes of these days, albeit with less detail than the September day for brevity. Table 4 shows the total daily source energy consumption estimated for the small and medium size office buildings for these days and Table 5 presents the estimated energy savings of the Optimal Control strategy compared to the three other control strategies during these same days.

The Optimal, Always-Bright, and Rule-Based control strategies all reached the same energy consumption on December 21 because the continuously cold outside temperature causes the ETFE cushions switch to the Always-Bright condition at all times to take the most advantage of sunlight for both daylight harvesting and heating. Similarly, on June 21, the Optimal, Always-Dark, and Rule-Based control strategies all reached to nearly the same results because with continuously high outside temperatures, the ETFE tends to switch to Always-Dark mode to decrease the cooling energy consumption as much as possible. Results from the Optimal Control strategy were slightly better than the Rule-Based and Always-Dark control strategies: approximately 2% and 1% lower energy consumption for the small office and medium size office buildings, respectively. Greater magnitudes of savings for the Optimal Control strategy are observed on March 21, which as a spring shoulder season day is closer to the September simulation day in that diurnal variations in ambient conditions provide greater potential for optimization.

4.5. Impacts of different temperature threshold values for the rule-based control

This section evaluates the impacts of different ambient temperature threshold values to switch the ETFE modes from dark mode to bright mode or vice versa in the Rule-Based Control strategy. An ambient temperature range of 11.6 °C to 18.6 °C with step size of 1°C was considered to assess the impacts of the switch temperature in addition to the originally considered 15.6 °C. Table 6 presents the results for estimated total daily source energy consumption for the small and medium size office building for all four simulation days considered earlier and under the different temperature threshold values for the Rule-Based Control strategy.

For the small office building, in Sep 30 as the representative of a shoulder season day, the minimum energy consumption occurs at a threshold of 15.6 °C (5.85×10^8 J). It is observed that with a deviation from this threshold temperature in either direction, the energy consumption on this simulation day would increase, for example by up to 3% for the lowest temperature thresholds and by up to 18% for the highest threshold. For the other simulation days of December 21, June 21 and March 21, the energy consumption for all temperature thresholds remains the same for this control strategy. The reason is that the temperature variation throughout in these days is consistently either above or below the thresholds defined in Table 6, which results in no dynamic changes of the ETFE status throughout the representative simulation days.

Conversely, for the medium size office building, the lowest energy consumption is achieved for the Rule-Based Control on September 30 with a switch mode temperature of 12.6 °C (6.42×10^9 J), increasing by up to 19% at the highest threshold temperature. The reason can be explained in Fig. 12 and Fig. 13, which show that the lighting energy consumption of the medium office core zone is considerably higher than the other zones due to its larger area. Consequently, switching the ETFE status from Always-Bright to Always-Dark does not change the total lighting energy consumption much, and while the heating energy consumption is also not very sensitive to Always-Bright or Always-Dark modes, the cooling energy consumption is more sensitive to the mode of operation. Thus, the cooling energy will be the most sensitive factor guiding the direction of problem. It is clear from Fig. 13 that in Always-Dark mode, the cooling energy of the perimeter zones are significantly lower compared to the Bright mode. This is why the lower ambient temperature threshold of 12.6 °C is the optimum threshold temperature compared to the default of 15.6 °C. Also, based on Table 2, for the medium office, the Always-Dark mode has lower energy consumption compared to the Rule-Based Control with 15.6 °C as the threshold temperature. It is noted that the threshold temperature would most likely be different for different office sizes, and the threshold temperature needs to be tuned for buildings with different envelope and geometry characteristics. Additionally, similar to the small office building, the energy consumption for all temperature thresholds remains the same for the other simulation days of December 21, June 21 and March 21. The result of this temperature threshold value analysis further illustrates that sometimes the Rule-Based Control or sequences of operation that are currently being applied in the industry perform worse than the optimal (or near optimal) control.

Table 7 summarizes the total daily source energy consumption for the medium size office building during the September simulation day for default and optimum thresholds based on the results of Table 6. Table 8 shows the associated daily savings for the two switch temperature values shown in Table 7. Based on Table 8, the amount of energy savings potential of the Optimal Control strategy compared to the Rule-Based Control strategy with default and optimum threshold temperatures in the medium office would be 3.7% and 1.9%, respectively.

Table 5
Total daily source energy savings from using the Optimal Control strategy compared to the three other strategies in the small and medium size office buildings for the 21st of December, June, and March.

Total daily source energy savings (%)						
Optimal Control savings compared to the other strategies	Small size office			Medium size office		
	Dec 21	June 21	March 21	Dec 21	June 21	March 21
vs. Always-Bright	0.0%	24.6%	9.9%	0.0%	19.1%	9.3%
vs. Always-Dark	6.7%	1.9%	14.4%	5.3%	1.1%	10.6%
vs. Rule-Based	0.0%	1.9%	9.9%	0.0%	1.1%	9.3%

4.6. Economic analysis

This section provides a brief assessment of the costs of installing and operating ETFE building façades compared to conventional construction, which is intended to provide some insight into the relative costs and benefits of this type of system.

4.6.1. Cost of ETFE inflating/switching action

This section estimates the annual energy cost of the inflating/switching action to change the ETFE status in the hypothetical small and medium size office buildings in Chicago, IL under assumptions of constant utility rates and Time-of-Use (TOU) utility rates. Table 9 shows the utility rate of constant and TOU programs for different Peak, Off-Peak and Super-Peak daily period (ComEd, n.d.).

The inflating action is done by constantly blowing air from the compressor into the ETFE chambers and the switching action is carried out by varying air flow and adjusting the air pressure in each cushion. By this adjustment, the internal layer changes their position inside the cushion and the status changes. Therefore, the annual energy cost for the inflating/switching action is estimated by expanding the ETFE inflating/switching cost of representative simulation days to represent their entire associated seasons and summing up the costs in each season to reach the annual cost. For the shoulder season, we used the daily cost of inflating/switching the ETFE status on the September 30 simulation day, which was already achieved through the Optimal Control schedule, and assumed this day replicated during each day of the shoulder season months including April, May, September, and October. This scenario was also used for the representative day of the winter season, December 21, which was assumed to represent each day in January, February, March, November, and December. To consider the summer season, the representative day of June 21 was used to assess energy consumption

Table 6
Total daily source energy consumption for the small and medium size office buildings under different temperature threshold for Rule-Based Control for the days under study.

Total daily source energy consumption (J)								
Temperature	Small size office				Medium size office			
	Sep 30	Dec 21	June 21	March 21	Sep 30	Dec 21	June 21	March 21
T = 11.6 °C	6.04×10^8	1.38×10^9	1.56×10^9	9.69×10^8	6.43×10^9	9.25×10^9	1.80×10^{10}	7.17×10^9
T = 12.6 °C	6.02×10^8	1.38×10^9	1.56×10^9	9.69×10^8	6.42×10^9	9.25×10^9	1.80×10^{10}	7.17×10^9
T = 13.6 °C	5.86×10^8	1.38×10^9	1.56×10^9	9.69×10^8	6.45×10^9	9.25×10^9	1.80×10^{10}	7.17×10^9
T = 14.6 °C	5.86×10^8	1.38×10^9	1.56×10^9	9.69×10^8	6.48×10^9	9.25×10^9	1.80×10^{10}	7.17×10^9
T = 15.6 °C	5.85×10^8	1.38×10^9	1.56×10^9	9.69×10^8	6.54×10^9	9.25×10^9	1.80×10^{10}	7.17×10^9
T = 16.6 °C	5.87×10^8	1.38×10^9	1.56×10^9	9.69×10^8	6.77×10^9	9.25×10^9	1.80×10^{10}	7.17×10^9
T = 17.6 °C	6.21×10^8	1.38×10^9	1.56×10^9	9.69×10^8	7.15×10^9	9.25×10^9	1.80×10^{10}	7.17×10^9
T = 18.6 °C	6.88×10^8	1.38×10^9	1.56×10^9	9.69×10^8	7.77×10^9	9.25×10^9	1.80×10^{10}	7.17×10^9

Table 7
Total daily source energy consumption for medium size office buildings during the September simulation day for default and optimum threshold temperature of Rule-Based Control.

Total daily source energy consumption, J		
Control Strategy	Rule-Based Control with default threshold temperature of 15.6 °C	Rule-Based Control with optimum threshold temperature of 12.6 °C
Rule-Based	6.54×10^9	6.42×10^9

and costs of each day in June, July, and August.

For the inflating/switching cost estimation, we used the recorded current data (Amps) of the compressors operating in the Kaplan Institute building at Illinois Institute of Technology to calculate the power/energy consumption of the compressors for dark and bright status, using the formula $P = \sqrt{3} \times V \times I \times pf$, where V is the voltage in Volts, I is the current in Amps and pf is the power factor, which we assumed to be 0.85 for three phase compressors. We then calculated the required power draw per square meter of ETFE envelope area (W/m^2) for each switching action between dark and bright status. Based on the optimal ETFE schedule that we estimated for each side of the building and the ETFE area for each of small and medium size office building, the power/energy consumption of the compressors to change the ETFE status is calculated for each representative day. This approach is simplistic and does not use daily data beyond the four simulation days but provides some insight into the potential magnitudes of inflating/switching energy costs throughout the year without having to run computationally expensive annual simulations.

Table 10 shows the estimated cost of inflating/switching the ETFE status using air compressor(s) for each of the shoulder, winter, and summer seasons, as defined, for both the small and medium size office buildings based on both utility rate assumptions. As it is observed in Table 10, for the constant utility rate, the cost for ETFE inflating/switching is highest in winter, followed by the shoulder and summer seasons. The reason for this hierarchy is due in part to the number of months that were considered for each season (i.e., 5 months for the winter season, 4 months for the shoulder season, and 3 months for the summer season), as well as differences in inflating/switching patterns.

Table 8
Total daily source energy savings from using the Optimal Control strategy compared to Rule-Based strategy with default and optimum threshold temperature in the medium size office building during the September simulation day.

Total daily source energy savings (%)		
Optimal Control savings compared to the Rule-Based control with different threshold temperatures	T = 15.6 °C	T = 12.6 °C
vs. Rule-Based	3.7%	1.9%

The total inflating/switching action cost for constant utility rate is estimated as $581 per year for the small office building and $3,435 per year for the medium size office building. For the TOU program, the cost is highest in the shoulder season, followed by the summer and winter seasons. It is interesting to observe that the winter season, which was the highest costly season in the constant rate program, is the cheapest season in the TOU program. The reason is due to lower numbers of switches in the winter along with the varying cost of utility rates in the TOU program that involves more off-peak usage. The total cost for inflating/switching under the TOU program is estimated as $336 per year for the small office building and $2,345 per year for the medium size office building. Therefore, based on these estimates, adoption of a TOU program could yield approximately 42% and 31% in annual cost savings for ETFE switching in the small and medium size office buildings, respectively.

4.6.2. Cost of ETFE compared to conventional construction

This section evaluates the total construction cost of switchable ETFE and its required equipment (e.g., compressor and piping), including the cost of purchase, labor for installation, and profit cost, and compares the cost with a conventional construction assembly, which is assumed to be a double-glazed curtain wall. The curtain wall is assumed to consist of two 3 mm clear glass layers with a 13 mm air gap between them with total assembly U-value of 2.73 W/m^2K, which is nearly the same U-value as the ETFE construction to provide a fair comparison. Each glass has solar transmittance of 0.837, visible transmittance of 0.898, and thermal conductivity of 0.9 W/m-K. Table 11 presents assumptions for the cost of construction including materials, compressors and air dryer, and piping for the ETFE enclosure. These costs were obtained by averaging the quoted costs from multiple original quotes for the ETFE enclosure on the Kaplan Institute building, provided by IIT's Facilities Department. Only material costs are shown for the assumed curtain wall assembly, which were estimated using RSMeans (RSMeans Online, n.d.) with the design documents for the Kaplan Institute building as a guide for sizing the conventional enclosure. For example, for piping, we considered the size of the pipes, which were designed exclusively for the Kaplan Institute building, and used that to evaluate the cost of piping assuming different lengths for the small and medium size office buildings. We assumed four compressors with 7.457 kW (10 HP) for each façade cardinal direction (i.e., north, east, south, ad west) of the medium size office building, and four compressors with 1.49 kW (2 HP) each for the small office building.

Table 9
Utility rate of constant and TOU programs for the city of Chicago, IL.

Utility rate program	Off-Peak (10 pm-6 am)	Peak (6 am-2 pm & 7 pm-10 pm)	Super peak (2 pm-7 pm)
Constant (¢/kWh)	5.847	5.847	5.847
Time-Of-Use (¢/kWh)	1.779	2.710	12.867

Table 10
Annual cost of ETFE inflating/switching action in different seasons for small and medium size office building based on two utility rate programs in Chicago, IL.

Cost of ETFE inflating/switching ($)								
Utility rate program	Small size office				Medium size office			
	Shoulder	Winter	Summer	Total	Shoulder	Winter	Summer	Total
Constant	$199	$222	$160	$581	$1,217	$1,220	$997	$3,435
TOU	$141	$96	$100	$336	$790	$934	$621	$2,345

Table 11
Cost estimation of ETFE and curtain wall construction along with annual site energy consumption for small and medium size office building.

Cost ($)					
Cost type	Item	Small size office		Medium size office	
		ETFE	Curtain wall	ETFE	Curtain wall
Capital	Materials, framing, and labor cost	$180,390	$329,230	$984,682	$1,797,148
	Compressor and air dryer	$11,100	–	$55,496	–
	Piping	$13,826	–	$75,728	–
	Total	$205,316	$329,230	$1,115,906	$1,797,148
Operational (Annual)	Inflating/switching (constant rate)	$581	–	$3,435	–
	Inflating/switching (TOU)	$336	–	$2,345	–
	Site energy consumption	$2,351	$3,750	$20,583	$30,848
	Total (constant rate)	$2,932	$3,750	$24,018	$30,848
	Total (TOU)	$2,687	$3,750	$22,928	$30,848

For compressor selection, we scaled the nominal compressor power based on the ETFE area used in the Kaplan Institute building as the reference and the ETFE areas used in small and medium size office buildings.

The main capital costs for ETFE construction refers to its material (including framing and labor costs), as the compressor and piping costs are negligible compared to the material cost. The total capital cost of the ETFE construction in the small office building is estimated as $180,390, which is 54% of the cost of the conventional curtain wall construction, estimated as $329,230. For the medium size office building, the total cost of ETFE construction is estimated to be $984,682, which is 62% of the cost of the conventional curtain wall construction, estimated as $1,797,148. Comparisons are proportionally different due to the scaling of the compressor power and cost based on the ETFE envelope area. It is also worth noting that since the major contribution of the costs refers to material, framing, and labor cost the exact cost of compressors and piping size estimation for small and medium size office will not significantly change the total capital cost for the ETFE construction.

The other category of costs is operational costs, which includes costs for heating, cooling, and lighting energy consumption for both façade types and for powering the inflating/switching action with the ETFE façade. It is noted that the inflating/switching cost for ETFE is based on both the constant utility rate and the TOU program. The total operational cost is estimated by adding the inflating/switching and site energy cost. For the small size office, the total energy cost for heating, cooling, lighting, and façade inflating/switching is estimated to be $2,932 with constant utility rate and $2,687 with TOU program for the ETFE façade and $3,750 for the curtain wall construction (no switching). For the medium size office, the total energy cost for heating, cooling, lighting, and façade inflating/switching is estimated to be $24,018 with constant utility rate and $22,928 with TOU program for the ETFE façade and $30,848 for the curtain wall (no switching). Thus, the total operational cost of the ETFE construction is estimated as 78% of curtain wall construction for both constant utility rate and TOU program in small size office while in the medium size office, the ETFE operational cost is about 72% and 74% of curtain wall construction for constant utility rate and TOU program, respectively. In summary, based on the provided cost estimation, the total construction cost of the ETFE enclosure is less expensive than the conventional curtain wall construction. And although the switchable ETFE enclosure uses compressors to keep them inflated and to change their dark/bright status, the total operational cost is also estimated to be lower than the conventional curtain wall construction because of the energy cost savings predicted from using the ETFE enclosure to dynamically change status.

5. Discussion

To our knowledge, this is the first study to consider the feasibility of optimally controlling switchable ETFE cushion façade positions. We demonstrate a novel co-simulation approach to identify Optimal Control strategy to minimize daily energy consumption for heating, cooling, and lighting on four simulation days representing four seasons by dynamically adjusting ETFE cushion positions. We demonstrate that the Optimal Control strategy results in energy savings of between 8% and 25% in the small office building model and between 4% and 22% in the medium size office model for shoulder season days, between 1.9% and 24.6% in the small office building and between 1.1% and 19.1% in the medium office building for the summer season day, and up to 6.7% in the small office building and up to 5.3% in the medium office building in the winter season day, depending on the reference control strategy.

One limitation of this study is the high computational run time of the simulation phase. The process of running the model through EnergyPlus and reading the output from the CVS file totally takes from 1.7 and 1.8 s for small and medium size office buildings. For optimization we used 50 search agents with 400 iterations, leading to 20,000 function evaluations, which means that each model takes about 8.5 h to be optimized. Future work should consider faster and more effective binary optimizer approaches to improve convergence speed and reduce computational time. Future work should also leverage parallelization of the simulator-optimizer framework to significantly reduce computational time. Since the defined problem in our case is a binary problem, another point worth discussing is related to the total possible solution of the problem. As we already discussed, there are 90 design variables/control nodes defined in our case (which can also vary based on user preference), while each variable has two status potentials (dark and bright), resulting in 2^{90} total possible solutions. Considering the runtime of each simulation as 1.7/1.8 s depending on the office size, methods such as exhaustive search/brute force in an effort to find the global solution would be infeasible.

Additionally, Section 4.6 summerized the economicl analysis, including the total capital and operational costs, for the ETFE

construction under consideration and the conventional curtain wall construction in both small and medium size office buildings. Also, ETFE construction offers other advantages that need to be considered. For example: (1) contrary to conventional construction assemblies, ETFE facades can have lower embodied energy and can be made of recycled materials; (2) they are very lightweight compared to glass (i.e., 1% the weight of glass and the glass frame), which can reduce structural costs elsewhere; (3) due to their non-stick surface, they are self-cleaning and have high corrosion resistance; (4) ETFE façades are very flexible and can be shaped into any curvatures to meet innovative building envelope designs; (5) the spectral distribution of visible light is near constant with minimal refraction, so the intensity and quality of colors are retained inside the building, contrary to many types of glass (Afrin, 2016); and (6) relevant to their adjustable building façades, the meet the future needs of a grid interactive efficient buildings (e.g., TOU or demand response programs), which is gaining support at federal agencies such as the U.S. Department of Energy (DOE) to shave the building electric grid and accommodate increases in intermittent renewable energy production.

Results of this Optimal Control investigation can be translated into the SOO for building automation systems. Future studies can extract the rules using different constraints and objectives from the schedules derived from the Optimal Control to present a rule for SOO, which could be used to inform ASHRAE Guideline 36 by adding a section of switchable ETFE structures. This addition enables ETFE manufacturers, architects, and engineers to directly apply higher performance SOO for these structures. Future work should consider other ETFE-related design variables, such as thermal/optical properties that may be different from those used herein.

Additionally, other than SOO, another way to implement the Optimal Control strategy to a real building would be real-time optimization. In this case, an energy model of a real building would be built and validated with measured data. In order to have a stream of real-time data, sensors should be installed in different zones to measure temperature, humidity, occupancy, lighting, etc., and the measured data along with online weather data would be saved in a database server. These data would then be used to overwrite the IDF file components with measured data in real-time. The revised IDF file and online weather data would be employed by MATLAB and EnergyPlus for optimization. After getting the results from the optimization, the status of the first control node of the sequence would be sent to BAS interface such as BACnet and would be implemented by the actuators (i.e., compressors in this case). There are also other practical frameworks such as Virtual Cybernetic Building Testbed (VCBT) (Bushby et al., 2010) developed by National Institute of Standard and Technology (NIST) and Building Operation TESTing (BOPTEST) (Blum et al., 2019) developed by Lawrence Berkeley National Laboratory (LBNL) that could be used as the interface between control hardware and building simulation programs to apply advance control strategies in real time control and optimization.

6. Conclusion

This work describes a feasibility study for the optimal control of switchable ETFE cushion façades using two case study buildings – a small and medium size office building – located in Chicago, IL USA. All sides of the building were assumed to utilize switchable ETFE, while only the west, south, and east façades were assumed to be optimally controlled based on feedback from the ambient environment. The problem of optimal control was discretized in time and converted to the non-linear binary optimization problem, which was solved by an advanced binary version of a swarm intelligence technique (Binary Particle Swarm Optimizer with V-Shape transfer function). An optimal schedule for ETFE actuators was derived to minimize total daily source energy use for heating, cooling, and lighting during four representative days, one for each season, to demonstrate the approach. The Optimal Control strategy utilized on a single shoulder season day (September 30) was estimated to yield daily source energy savings of 8.2%, 11.1%, and 25.5% compared to the Rule-Based (as the current state-of-the-art strategy), Always-Dark, and Always-Bright strategies for the small office building and savings of 3.7%, 2.2%, and 21.9% compared to the Rule-Based, Always-Dark, and Always-Bright strategies for the medium size office building. Savings potentials were similar during a spring solstice day (March 21), but lower for more extreme conditions during summer (June 21) and winter (December 21) due to limited diurnal variations in ambient conditions. The economic analysis also revealed that the capital cost of ETFE construction is estimated as 54% for small size office building and 64% for medium size office building compared to the conventional curtain wall construction. The operational cost of ETFE construction is calculated as 78% conventional curtain wall construction in small size office building for both constant utility rate and Time-of-Use (TOU) program. In the medium size office building, the ETFE operational cost is about 72% and 74% of curtain wall construction for constant utility rate and TOU program, respectively. To the best of the authors' knowledge, this is the first study of which we are aware to provide control schedules cofor operating dynamic ETFE cushion façades.

Funding

This study was supported and funded by an ASHRAE New Investigator Award to Mohammad Heidarinejad.

Declaration of Competing Interest

The authors declare the following financial interests/personal relationships which may be considered as potential competing interests: This study was supported and funded by an ASHRAE New Investigator Award to Mohammad Heidarinejad.

Acknowledgement

We would like to thank the IIT Planning, Design, + Construction Department especially Colette Porter, AVP PD+C and Thomas Henehan, Senior Project Manager PD+C for their support and providing materials for cost estimation of ETFE enclosure assembly at the Kaplan Institute Building. In addition, authors would like to thank Lawrence E. Dorn, Adjunct Professor at Illinois Tech, for his assistance with the cost estimation, Sachin Anand, Principal at dbHMS, for his support with the ETFE design of Kaplan Institute of building, and two anonymous reviewers for sharing their constructive feedback.

References

Afrin, S., 2016. Thermal Performance Analysis of ETFE-foil Panels and Spaces Enclosed with ETFE-foil Cushion Envelope [Doctoral Thesis]. University of Nottingham.

ASHRAE, 2009. ANSI/ASHRAE/USGBC/IES Standard 189.1-2009: Standard for the Design of High-Performance Green Buildings Except Low-Rise Residential Buildings (ASHRAE 189.1). ASHRAE.

ASHRAE, 2018. ASHRAE Guideline 36-2018: High-Performance Sequences of Operation for HVAC Systems. American Society of Heating, Refrigerating and Air-Conditioning Engineers, Inc.

Berger, J., Mendes, N., 2017. An innovative method for the design of high energy performance building envelopes. Appl. Energy 190, 266–277. https://doi.org/10.1016/j.apenergy.2016.12.119.

Biloria, N., Sumini, V., 2009. Performative Building Skin Systems: A Morphogenomic Approach Towards Developing Real-Time Adaptive Building Skin Systems. Int. J. Architec. Comput. 7 (4).

Blum, D., Jorissen, F., Huang, S., Chen, Y., Arroyo, J., Benne, K., Li, Y., Gavan, V., Rivalin, L., Helsen, L., Vrabie, D., Wetter, M., Sofos, M., 2019. Prototyping the BOPTEST Framework for Simulation-Based Testing of Advanced Control Strategies in Buildings. In: IBPSA Building Simulation Conference 2019.

Bushby, S.T., Galler, M.A., Milesi-Ferretti, N.S., Park, C.D., 2010. The Virtual Cybernetic Building Testbed-A Building Emulator. ASHRAE Trans. 116 (1).

Chan, K.T., Chow, W.K., 1998. Energy impact of commercial-building envelopes in the sub-tropical climate. Appl. Energy 60 (1), 21–39. https://doi.org/10.1016/S0306-2619(98)00021-X.

Charbonneau, L., Polak, M.A., Penlidis, A., 2014. Mechanical properties of ETFE foils: Testing and modelling. Constr. Build. Mater. 60, 63–72. https://doi.org/10.1016/j.conbuildmat.2014.02.048.

Cheung, C.K., Fuller, R.J., Luther, M.B., 2005. Energy-efficient envelope design for high-rise apartments. Energy Build. 37 (1), 37–48. https://doi.org/10.1016/j.enbuild.2004.05.002.

ComEd., n.d. Time-of-Day Pricing | ComEd—An Exelon Company. Retrieved January 10, 2021, from https://www.comed.com/WaysToSave/ForYourHome/Pages/TimeofDayPricing.aspx.

Cremers, J., Marx, H., 2016. Comparative Study of a New IR-absorbing Film to Improve Solar Shading and Thermal Comfort for ETFE Structures. Procedia Eng. 155, 113–120. https://doi.org/10.1016/j.proeng.2016.08.012.

Cremers, J., Marx, H., 2017. Improved daylight comfort by a new 3D-foil that allows to trade off solar gains and light individually. VIII International Conference on Textile Composites and Inflatable Structures.

Deru, M., Torcellini, P., 2007. Source Energy and Emission Factors for Energy Use in Buildings (Technical Report NREL/TP-550-38617). National Renewable Energy Laboratory.

Deru, Michael, Field, K., Studer, D., Benne, K., Griffith, B., Torcellini, P., Liu, B., Halverson, M., Winiarski, D., Rosenberg, M., Yazdanian, M., Huang, J., Crawley, D., 2011. U.S. Department of Energy Commercial Reference Building Models of the National Building Stock (Technical Report NREL/TP-5500-46861). NREL.

DOE, 2019. Grid-interactive efficient buildings technical report series: Windows and opaque envelope. U.S. Department of Energy.

Ellis, P.G., Torcellini, P.A., Crawley, D., 2008. Simulation of Energy Management Systems in EnergyPlus (NREL/CP-550-41482). National Renewable Energy Lab (NREL), Golden, CO (United States).

Emary, E., Zawbaa, H.M., Hassanien, A.E., 2016. Binary grey wolf optimization approaches for feature selection. Neurocomputing 172, 371–381. https://doi.org/10.1016/j.neucom.2015.06.083.

EnergyPlus, 2000. Input Output Reference. The Encyclopedic Reference to EnergyPlus Input and Output.

EnergyPlus, 2020. Weather Data Download—Chicago-OHare Intl AP 725300 (TMY3). https://energyplus.net/weather-location/north_and_central_america_wmo_region_4/USA/IL/USA_IL_Chicago-OHare.Intl.AP.725300_TMY3.

Flor, J.-F., Liu, D., Sun, Y., Beccarelli, P., Chilton, J., Wu, Y., 2018. Optical aspects and energy performance of switchable ethylene-tetrafluoroethylene (ETFE) foil cushions. Appl. Energy 229, 335–351. https://doi.org/10.1016/j.apenergy.2018.07.046.

Poirazis, Harris, Kragh, Mikkel, Hogg, Charlie, 2009. Energy modelling of ETFE membranes in building applications. In: 11th International IBPSA Conference. Building Simulation 2009, Glasgow, Scotland.

Hu, J., Chen, W., Zhao, B., Yang, D., 2017. Buildings with ETFE foils: A review on material properties, architectural performance and structural behavior. Constr. Build. Mater. 131, 411–422. https://doi.org/10.1016/j.conbuildmat.2016.11.062.

Huang, J., Franconi, E., 1999. Commercial heating and cooling loads component analysis No. 37208. Lawrence Berkeley National Laboratory.

Huang, J., Hanford, J., Fuqiang, Y., 1999. Residential heating and cooling loads component analysis No. 44636. Lawrence Berkeley National Laboratory.

Kennedy, J., Eberhart, R., 1997. A discrete binary version of the particle swarm algorithm. Proceedings of the IEEE International Conference on Computational Cybernetics and Simulation.

Li, T., Zhai, Y., He, S., Gan, W., Wei, Z., Heidarinejad, M., Dalgo, D., Mi, R., Zhao, X., Song, J., Dai, J., Chen, C., Aili, A., Vellore, A., Martini, A., Yang, R., Srebric, J., Yin, X., Hu, L., 2019. A radiative cooling structural material. Science 364 (6442), 760. https://doi.org/10.1126/science.aau9101.

Maywald, C., 2019. Coating of ETFE – Solar Shading for Architectural Applications. The TensiNet Symposium.

Menéndez, A., Martínez, A., Santos, A., Ruiz, B., Moritz, K., Klein, I., Díaz, J., Lagunas, A. R., Sauermann, T., Gómez, D., 2018. A multifunctional ETFE module for sustainable façade lighting: Design, manufacturing and monitoring. Energy Build. 161, 10–21. https://doi.org/10.1016/j.enbuild.2017.12.023.

Mirjalili, S., Lewis, A., 2013. S-shaped versus V-shaped transfer functions for binary Particle Swarm Optimization. Swarm Evol. Comput. 9, 1–14. https://doi.org/10.1016/j.swevo.2012.09.002.

Mu, C., Liu, W., Xu, W., 2018. Hierarchically Adaptive Frequency Control for an EV-Integrated Smart Grid With Renewable Energy. IEEE Trans. Ind. Inf. 14 (9), 4254–4263. https://doi.org/10.1109/TII.2018.2846545.

Mu, C., Zhang, Y., Jia, H., He, H., 2020. Energy-Storage-Based Intelligent Frequency Control of Microgrid With Stochastic Model Uncertainties. IEEE Trans. Smart Grid 11 (2), 1748–1758. https://doi.org/10.1109/TSG.2019.2942770.

Pal, A., Maiti, J., 2010. Development of a hybrid methodology for dimensionality reduction in Mahalanobis-Taguchi system using Mahalanobis distance and binary particle swarm optimization. Expert Syst. Appl. 37 (2), 1286–1293. https://doi.org/10.1016/j.eswa.2009.06.011.

Pérez-Lombard, L., Ortiz, J., Pout, C., 2008. A review on buildings energy consumption information. Energy Build. 40 (3), 394–398. https://doi.org/10.1016/j.enbuild.2007.03.007.

Robinson-Gayle, S., Kolokotroni, M., Cripps, A., Tanno, S., 2001. ETFE foil cushions in roofs and atria. Constr. Build. Mater. 15 (7), 323–327. https://doi.org/10.1016/S0950-0618(01)00013-7.

RSMeans Online, n.d., Retrieved January 10, 2021, from https://www.rsmeansonline.com/.

Sadineni, S.B., Madala, S., Boehm, R.F., 2011. Passive building energy savings: A review of building envelope components. Renew. Sustain. Energy Rev. 15 (8), 3617–3631. https://doi.org/10.1016/j.rser.2011.07.014.

Tang, H., Zhang, T., Liu, X., Liu, X., Xiang, X., Jiang, Y., 2018. On-site measured performance of a mechanically ventilated double ETFE cushion structure in an aquatics center. Sol. Energy 162, 289–299. https://doi.org/10.1016/j.solener.2018.01.042.

Zeng, X.-P., Li, Y.-M., Qin, J., 2009. A dynamic chain-like agent genetic algorithm for global numerical optimization and feature selection. Neurocomputing 72 (4), 1214–1228. https://doi.org/10.1016/j.neucom.2008.02.010.

Zhai, Z., 2003. Developing an integrated building design tool by coupling building energy simulation and computational fluid dynamics programs [PhD thesis]. Massachusetts Institute of Technology.

Zhao, B., Chen, W., Hu, J., Chen, J., Qiu, Z., Zhou, J., Gao, C., 2016. Mechanical properties of ETFE foils in form-developing of inflated cushion through flat-patterning. Constr. Build. Mater. 111, 580–589. https://doi.org/10.1016/j.conbuildmat.2016.01.050.

Zhao, B., Hu, J., Chen, W., Chen, J., Jing, Z., 2020. Uniaxial tensile creep properties of ETFE foils at a wide range of loading stresses subjected to long-term loading. Constr. Build. Mater. 253, 119112 https://doi.org/10.1016/j.conbuildmat.2020.119112.